

Z-Stacking of Single Plane Digital Widefield Fluorescent Images

Using the Agilent BioTek Cytation cell imaging multimode readers for deconvoluted, stacked images of 3D cellular structures

Authors

Brad Larson and
Peter Banks, PhD
Agilent Technologies, Inc.

Abstract

Three-dimensional (3D) cellular models have the potential to become a fundamental research tool in cell biology. This is because cell culture performed in this manner re-establishes cell-cell and cell-extracellular matrix interactions that mirror what's seen within real tissues. Histology slides, containing tissue samples mounted onto microscope slides, also continue to be an important research and diagnostic method in the clinic and laboratory. These multidimensional cell structures present complications for optical microscopy due to their thickness in the Z-axis. This application note presents a method to capture and project multiple single z-plane images using digital widefield microscopy.

Introduction

Z-stacking (also known as focus stacking) is a digital image-processing method which combines multiple images taken at different focal distances to provide a composite image with a greater depth of field (e.g., the thickness of the plane of focus) than any of the individual source images.^{1,2} It is useful for capturing in-focus images of objects under high magnification as depth of field (DOF) decreases with magnification primarily because microscope objectives with higher magnification have typically higher numerical apertures (NA). According to the Shillaber equation, DOF relates to NA for a given wavelength of light (λ) and medium refractive index (n):

$$\text{DOF} = \frac{\lambda \sqrt{n - (NA)^2}}{(NA)^2}$$

Table 1 illustrates this concept for a series of commercially available microscope objectives using 500 nm light and air as the medium (n = 1.00) between microscope objective and object.

Table 1. Relationship between magnification, numerical aperture, and depth of field.

Magnification	Numerical Aperture	Depth of Field (μm)
4x	0.10	50
10x	0.25	7.7
20x	0.40	2.9
40x	0.65	0.9
60x	0.85	0.36
100x	0.95	0.17

The dimensions of a typical mammalian cell (~ 50 μm) are only within the depth of field (in focus axially) using a 4x microscope objective. Magnification of 4x is inadequate to provide subcellular resolution in either axial or longitudinal axes, thus localization of structures of interest within the cell through its width requires use of higher magnification and means of removing out of focus objects.

This can be done using confocal microscopy where the field of view is restricted both axially and longitudinally, such as in a pin hole camera, so that in-focus slices of the object can be acquired and z-stacked to form a composite 3D image of the object. However, because the excitation light illuminates the entire structure, photobleaching and phototoxic effects extend to all planes. While the lack of longitudinal restriction seen in widefield microscopy helps to eliminate these complications, parts of the object will appear in focus and parts out of focus. In this case, z-stacking is still possible, but requires the use of projection, a technique to get rid of out-of-focus information

by applying a mathematical algorithm. This provides sharper images that can be combined to yield more realistic 3D impressions of the structure of interest. This application note demonstrates this technique using Agilent BioTek Gen5 Image+ data analysis software to perform z-stacking of images of a 3D spheroidal cellular structure, as well as a mouse kidney section.

Materials and methods

Materials

Cells

MDA-MB-231 GFP cells (part number AKR-201) were purchased from Cell Biolabs, Inc. (San Diego, CA). Human neonatal dermal fibroblasts expressing RFP (part number cAP-0008RFP) were purchased from Angio-Proteomie (Boston, MA). Both cell types were propagated in Advanced DMEM medium (part number 12491-015) plus fetal bovine serum (FBS), 10% (part number 10437-028) and pen-strep-glutamine, 1x (part number 10378-016) each from Life Technologies (Carlsbad, CA).

Histology slide

FluoCell prepared slide #3 (part number F-24630), containing a mouse kidney section stained with Alexa Fluor 488 wheat germ agglutinin (W-11261), Alexa Fluor 568 phalloidin (A-12380) and DAPI (D-1306) was purchased from Life Technologies (Carlsbad, CA).

Reagents

Hoechst 33342 (part number 14533) was purchased from Sigma-Aldrich (St. Louis, MO).

Agilent BioTek Cytation cell imaging multimode reader

The Cytation cell imaging readers combine automated digital microscopy and conventional multimode microplate detection providing rich phenotypic cellular information and well-based quantitative data. With special emphasis on live cell assays, the instruments feature temperature control, CO₂/O₂ gas control, and dual injectors for kinetic assays.

Agilent BioTek Gen5 image+ data analysis software

Gen5 Image+ software controls the operation of the Cytation cell imaging multimode reader for both automated digital microscopy and PMT-based microplate reading. Image acquisition is completely automated from sample translation, focusing, and exposure control. Users can also optimize and automate acquisition of images through 3D cellular structures or tissue, as well as creation of the final Z projection.

Corning spheroid microplates

Corning 96-well black, clear-bottom spheroid microplates (part number 4520) are coated with the ultra-low attachment surface, which is a noncytotoxic, and biologically inert covalently bonded hydrogel that prevents cell attachment. Novel well geometry aids spheroid formation in the center of each well.

Each microplate contains an optically clear round bottom, which is ideal for cellular imaging, as well as a black, opaque body that prevents cross talk.

Methods

Cell preparation and spheroid formation

MDA-MB-231 and fibroblast cells were harvested and diluted to a concentration of 5.0×10^4 cells/mL in complete medium. The two volumes were combined to create final concentrations of 2.5×10^4 cells/mL for each cell type. 100 μ L of cell suspension was then pipetted to appropriate wells. Following dispensing, the plate was placed at 37 °C/5% CO₂.

Image-based spheroid formation monitoring

Spheroid formation was monitored every 24 hours. The plate was placed into the Cytation, previously set to 37 °C/5% CO₂ using Agilent BioTek Gen5 data analysis software as well as a gas control module. Focusing was performed using the brightfield channel. The typical cell aggregation period for the combined cell types was 48 hours.

Creation of z-stacked images

In the imaging procedure read step, selection of objective, imaging channel, and exposure settings is performed in a manner similar to that for single image set capture. Image Z-Stack is then selected (Figure 1). The number of slices, or images taken through the structure, can be manually chosen depending on the definition desired. Step size is the distance in μ m that the objective will move in the Z-axis between each captured image. The default value is the depth of field for the objective chosen, 2.5x: 68 μ m; 4x: 53 μ m; 10x: 9 μ m; 20x: 4 μ m; 40x: 2 μ m; 60x: 1 μ m, which can also be manually adjusted should a higher number of slices be desired.

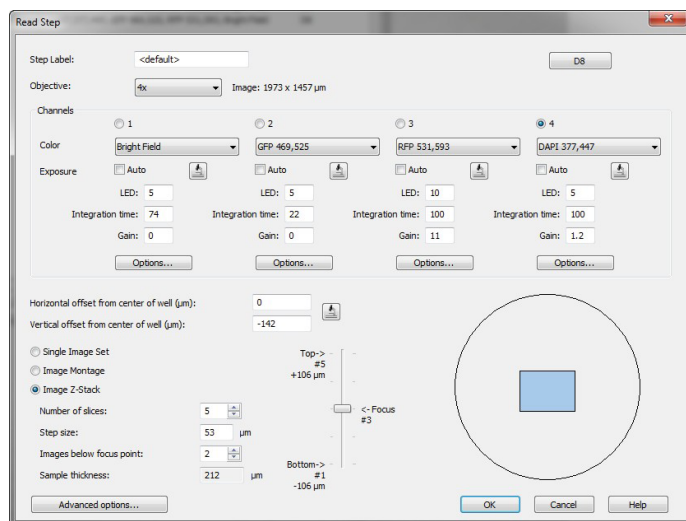


Figure 1. Agilent BioTek Gen5 2.07 image z-stack read step.

To determine the sample thickness and number of slices required to image through the complete structure, it is recommended to select manual imaging with one of the channels to be used. Auto Focus is selected to allow the Cytation to focus on a point within the structure. The focal height is then changed manually in each direction of the Z-axis to the point where a portion of the spheroid or tissue remains in focus (Figure 2).

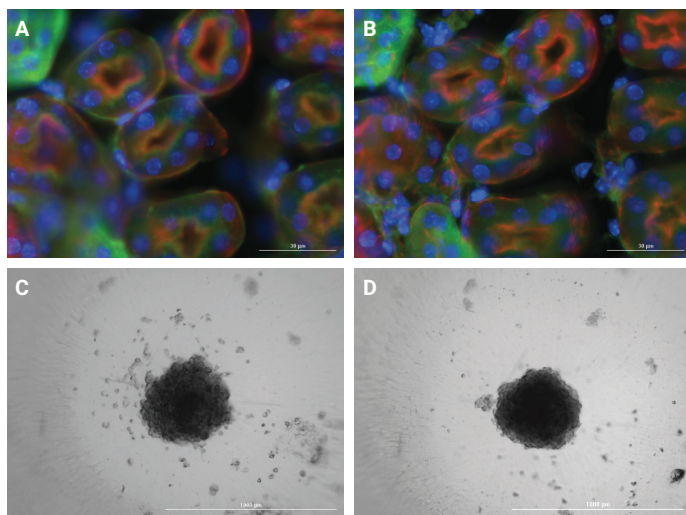


Figure 2. Manual determination of sample thickness. Object thickness determined for tissue (A and B) and spheroid (C and D) samples by finding top and bottom focal planes using manual imaging.

The total distance traveled from one point to the other is the sample thickness. This process is repeated to determine the typical focal height and distance traveled above and below the initial focal plane to reach each edge of the structure. Upon completion, manual imaging can then be closed. Using the gathered information, values are entered into the read step for **Number of slices**, **Step size**, and **Images below focus point** that equal the typical sample thickness, and also help to ensure that images are captured throughout the 3D cellular structure or tissue. Automated imaging can then be performed.

Z projection creation

Following capture of the z-stacked images, projection can be completed by performing a Z Projection data reduction step (Figure 3). Individual imaging channels can be chosen for inclusion in the projected image. The top and bottom image slices to use can be optimized to guarantee that the most in-focus image is created. Multiple projection methods exist which incorporate different algorithms for selecting the most in-focus portion of the z-stacked images. The method providing the desired projection may vary depending on the images captured and the final analysis required.

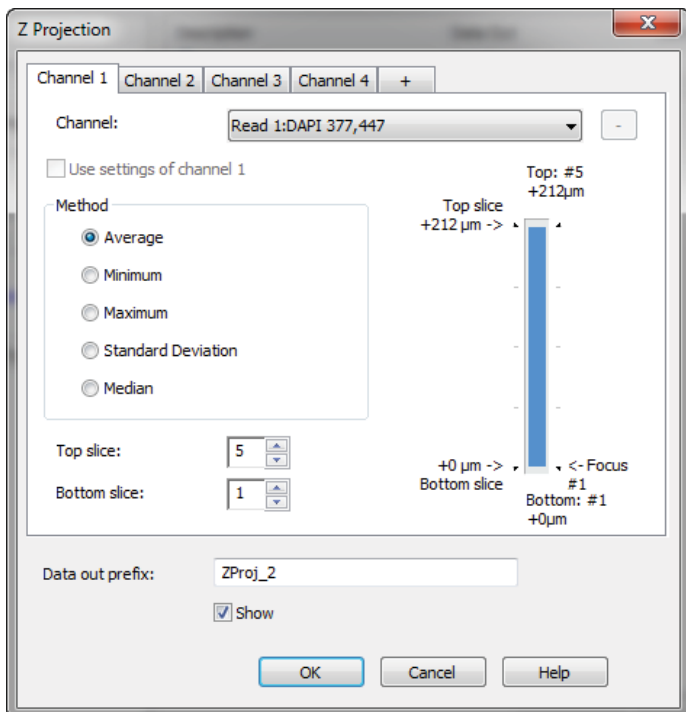


Figure 3. Set up of z projection data analysis.

If more imaging channels are to be included in the projection (Figure 4), subsequent channel tabs can be selected. The parameters can be kept consistent with those used for the initial channel, or can also be changed if necessary.

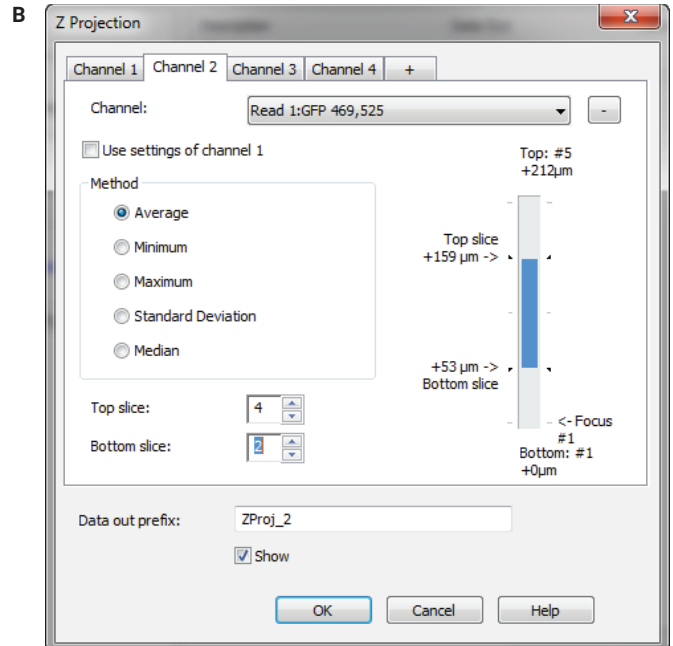
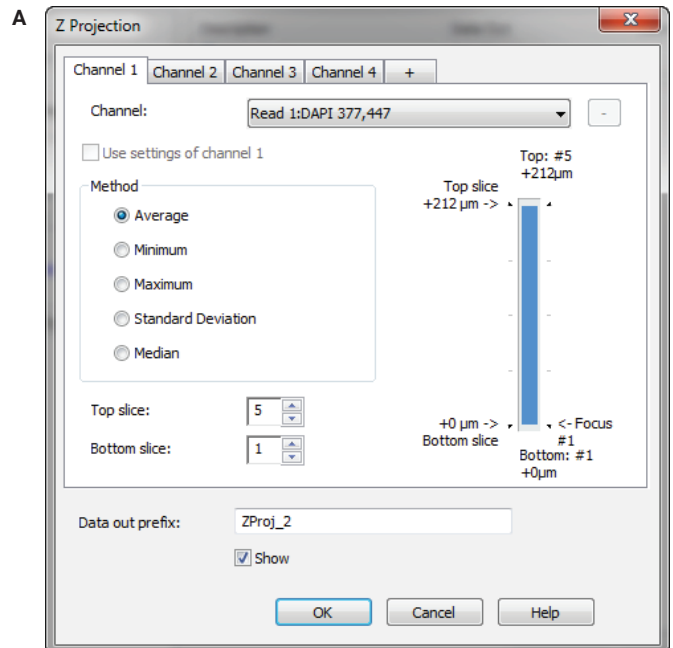


Figure 4. Subsequent imaging channel z projection optimization. Settings for more imaging channels to be included in Z Projection can be kept similar to that of Channel 1 (A) or re-optimized (B).

Results and discussion

Z-stack imaging of tissue samples

Visualization and analysis of tissue samples many times requires the incorporation of high magnification objectives in order to examine subcellular structures. However, tissue slices fixed onto histology slides can be tens of microns thick. As the depth of field of higher power objectives, such as 40x or 60x, is only 2 or 1 micron, respectively, there is a high probability that portions of the image will be out of focus. This is illustrated by the three single z-plane images, captured using a 60x objective (Figures 5A to 5C), where nuclei and other structures are clearly out of the focal plane. This issue is eliminated by stacking and projection of the collected images (Figure 5D), allowing for accurate visualization of the tissue.

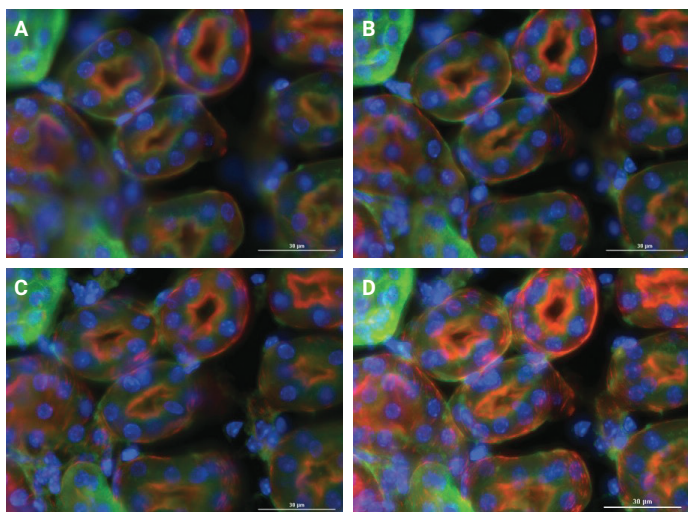


Figure 5. Single plane and z-stacked tissue images. (A to C) Images of mouse kidney section captured at individual z-planes using 60x objective. (D) Final z-stacked image following projection.

Spheroid image projection

Similar to histology samples, spheroids and tumoroids can be hundreds of microns in diameter. Experimental analysis of the effects that a potential drug candidate has on these structures, depending on the assay and test being performed, can many times be accomplished using single plane imaging. However, this is not always the case, and a final image showing improved cellular definition may be necessary. This is true when there is a desire to see the distribution of cocultured tumor and stromal cells within a formed spheroid (Figure 6). By following the process outlined, single plane images showing only partial cellular definition (Figures 6A to 6C) can again be projected to provide clear visualization.

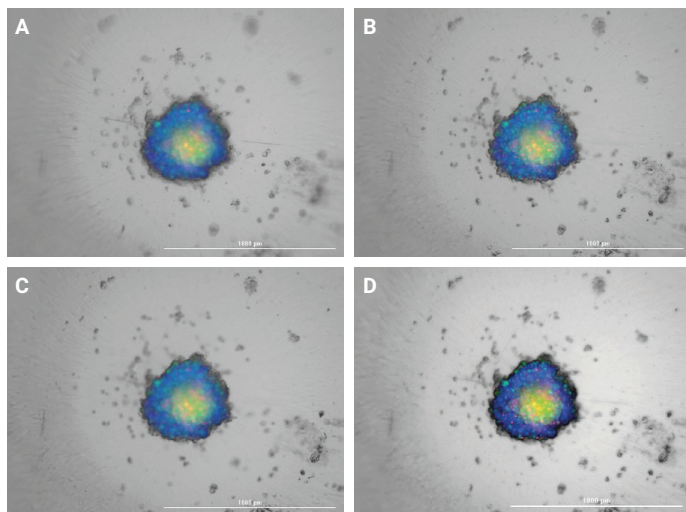


Figure 6. Single plane and z-stacked images of cocultured tumoroid structure. (A to C) Images of tumoroid captured at individual z-planes using 4x objective. (D) Final z-stacked image following projection. Image overlay shown using the following channels: Brightfield; GFP for identification of MDA-MB-231 cells; RFP for identification of fibroblasts; DAPI for identification of Hoechst 33342 stained nuclei.

Cellular analysis of projected images

Cellular analysis of 3D cellular structures can also be improved through the incorporation of a projected image. A prime example is the quantification of 3D tumor invasion. As the matrix, formed in the bottom of a microplate well, also has a certain depth, cells can invade not only in the X- and Y-axis but in the Z-axis as well. Therefore an accurate determination of the extent of invasion may not be possible using single plane images as out of focus cells do not always meet the analysis criteria (Figures 7A to 7C). A projected image that provides a clear picture of all portions of the invading structure then allows for precise conclusions to be drawn (Figures 7D and 7E).

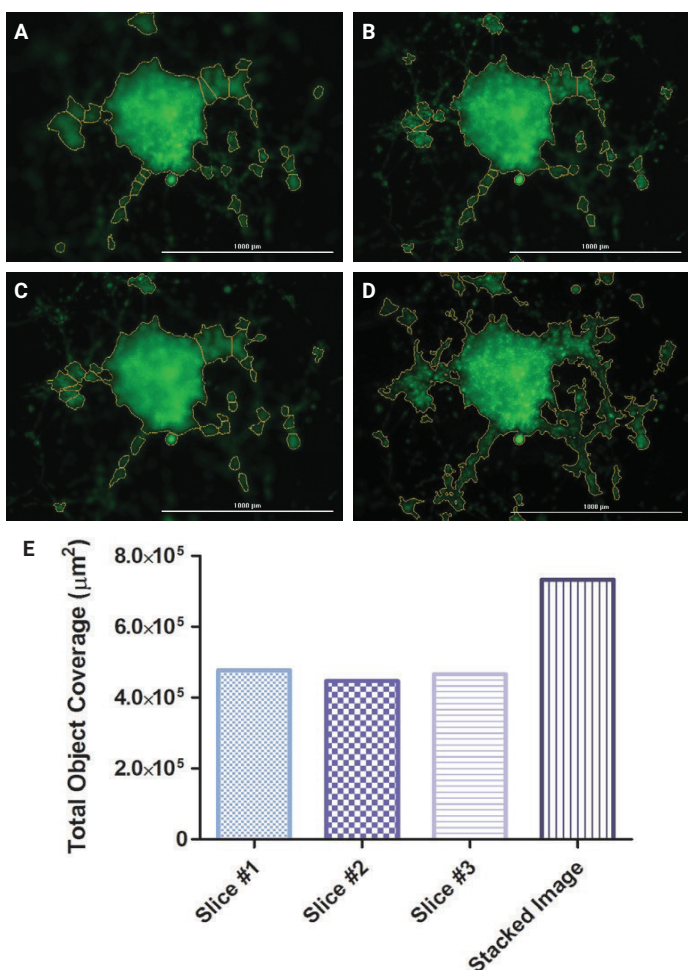


Figure 7. Single plane and z-stacked images of 3D MDA-MB-231 tumor invasion. (A to C) Images captured at individual z-planes using 4x objective. (D) Final z-stacked image following projection. GFP imaging channel used for identification of MDA-MB-231 cells. (E) Total area coverage of objects identified using cellular analysis on single slice and projected images.

Conclusion

Optical microscopy is one of the principal tools for analyzing cells, tissues, and complex models of cellular function, such as 3D models. Often high-resolution analysis is desired which requires high magnification microscope objectives with limited depths of field causing portions of specimens with considerable depth to be out of focus. This application note demonstrates this problem with fluorescent probes used for imaging both spheroids and tissues. Qualitatively, the images are less than desirable. Quantitatively, cellular analysis tends to underassess phenotypes. By acquiring z-stacks of images and performing z-projection image processing through Agilent BioTek Gen5 Image+, composite z-projected images demonstrate in-focus features and a more representative assessment of phenotype can be achieved.

References

1. Johnson, D. How to Do Everything: Digital Camera [Online]; *McGraw Hill Professional: New York*, **2008**; 336. http://books.google.com/books?id=h15xmx3ma2cC&q=inauthor:%22Dave+Johnson%22&dq=inauthor:%22Dave+Johnson%22&hl=en&sa=X&ei=ihtdcU sj_HM_ okAeuloHQBA&ved=0CGkQ6AEwCA (accessed October 14, 2013).
2. Ray, S. F. Applied Photographic Optics, Third Edition; *Focal Press: Oxford*, **2002**, 231–232.

www.agilent.com/lifesciences/biotek

For Research Use Only. Not for use in diagnostic procedures.

RA44411.596099537

This information is subject to change without notice.

© Agilent Technologies, Inc. 2022
Printed in the USA, August 9, 2022
5994-3349EN